energies

MDPI

Article

Influence of Passivation and Solar Cell Configuration on the Electrical Parameter Degradation of Photovoltaic Modules

Izete Zanesco *, Adriano Moehlecke, Jeferson Ferronato, Moussa Ly, João Victor Zanatta Britto, Bruno Inácio da Silva Roux Leite and Taila Cristiane Policarpi

Solar Energy Technology Nucleus (NT-Solar), School of Technology, Pontifical Catholic University of Rio Grande do Sul (PUCRS), Porto Alegre 90619-900, RS, Brazil; moehleck@pucrs.br (A.M.); jeferronato@hotmail.com (J.F.); moussa.ly@pucrs.br (M.L.); joao.britto@edu.pucrs.br (J.V.Z.B.); bruno.leite@edu.pucrs.br (B.I.d.S.R.L.); tailapolicarpi@gmail.com (T.C.P.)

* Correspondence: izete@pucrs.br

Abstract: This article analyses and compares the influence of p-type Cz-Si solar cells produced with and without Al-BSF and silicon oxide passivation on the degradation of the electrical parameters of PV modules, after 77 months under operating conditions in a PV system. Solar cells were manufactured at a pilot plant-scale facility, and 32 PV modules with silicon oxide passivated emitter and Al-BSF solar cells were assembled. The other group was composed of 28 PV modules produced with n^+pn^+ solar cells. The I–V curves of the PV modules were measured under standard test conditions before and after 77 months of exposure. In both groups, the short-circuit current presented higher degradation, and the open-circuit voltage showed low reduction. However, the degradation of these electrical parameters was lower in PV modules assembled with a passivated emitter and Al-BSF solar cells. Consequently, the power degradation rate of PV modules with passivated emitter n^+pp^+ and n^+pn^+ solar cells was 0.29% and 0.66% per year, respectively. The milky pattern was observed at the edge of all solar cells and was related to titanium dioxide antireflective coating modification and laser isolation processing.

Keywords: degradation rate; PV modules; silicon solar cell technology

check for updates

Citation: Zanesco, I.; Moehlecke, A.; Ferronato, J.; Ly, M.; Britto, J.V.Z.; Leite, B.I.d.S.R.; Policarpi, T.C. Influence of Passivation and Solar Cell Configuration on the Electrical Parameter Degradation of Photovoltaic Modules. *Energies* **2024**, *17*, 832. https://doi.org/10.3390/en17040832

Academic Editor: Philippe Leclère

Received: 22 December 2023
Revised: 16 January 2024
Accepted: 22 January 2024
Published: 9 February 2024

Copyright: © 2024 by the authors. Licensee MDPI, Basel, Switzerland. This article is an open access article distributed under the terms and conditions of the Creative Commons Attribution (CC BY) license (https://creativecommons.org/licenses/by/4.0/).

1. Introduction

In recent decades, the standard technology was phosphorus emitter and aluminum back surface field (Al-BSF) silicon solar cells. The market share of Al-BSF solar cells was 80% in 2016 [1] but is lower than 3% nowadays [2]. Currently, approximately 300 MW [3] of PV modules manufactured with this solar cell structure are installed in photovoltaic (PV) systems in different countries, and these modules operate under different climate conditions and are exposed to a range of solar irradiation levels.

The passivated emitter and rear solar cell (PERC) was developed in the 80s and 90s [4–6], and three decades were needed to achieve an industrially cost-effective process [4]. The solar cell efficiency was improved from around 20% (Al-BSF in 2017) to 23% with PERC technology and p-type Czochralski silicon (Si-Cz) wafers [1,2]. Currently, the market share of p-type PERC solar cells is higher than 80% [2]. The PERX family comprises the PERC, PERL (passivated emitter and rear locally diffused), PERT (passivated emitter and rear totally diffused) and PERF (passivated emitter and rear floating junction) solar cells. The main feature of the PERX configurations is the passivation in the rear face with a dielectric material to reduce the minority charge carrier recombination and improve the reflectance [7].

As a consequence of the silicon solar cell technology progress and the use of new materials to produce photovoltaic modules [8], different devices are operating in PV systems. The degradation of these devices is related to the solar cell configuration and processing, ethylene vinyl acetate (EVA) encapsulant, interface of the EVA and antireflective coating of

the solar cells, and backsheet and front materials, among other factors. To investigate the silicon substrate influence on the degradation rate, PV modules with upgraded metallurgical grade silicon (UMG-Si) solar cells were manufactured. A similar initial degradation rate to that produced with multicrystalline silicon [9] was found, indicating that the higher impurity of 99.9999% (6N) in the UMG-Si substrate does not affect the rate of aging. Moreover, the operating and weather conditions affect the degradation rate and can produce failures in PV modules [10–17].

The definitions of degradation and failure/defect in a PV module are not clearly reported in the literature [17]. Degradation can be defined as a change in the performance of the PV module [18,19], which produces maximum power output losses and occurs when the PV module is exposed to outdoor or operating conditions. The International Energy Agency (IEA) defines the term defect as anything in a PV module that is different from expected. The failures can be classified as infant, midlife and wear-out considering the occurrence time. The most typical failures are caused by diode or junction box defects, cell or string interconnection faults, cracked solar cells, corrosion of interconnections or solar cells, backsheet failure or burning, glass breakage, frame loosening and other failures. The importance of a specific failure can be ranked as having a high, medium or low occurrence probability and severity [17]. These PV module defects and the methods for detection are described in the literature [17,20].

The aging of PV modules can be related to EVA yellowing, light-induced degradation (LID), potential-induced degradation (PID), light-enhanced temperature-induced degradation (LeTID), delamination, antireflective coating modification, moisture penetration and other factors. Light-induced degradation occurs in p-type Cz-Si solar cells and is related to the oxygen and boron concentration in the substrate. As a result, the LID effect causes a reduction in the minority carrier lifetime [7]. Studies were developed to analyze the LID from the bulk lifetime in p-type silicon solar cells [21,22]. Another mechanism is light-enhanced temperature-induced degradation, which does not have a clear dependency on the oxygen in bulk, because LeTID was observed in solar cells produced with both Cz-Si and float-zone silicon wafers [7]. This degradation may be related to the materials and processes used to manufacture the solar cells. Specifically, in boron-doped substrate, the oxygen-related degradation can be enhanced by the materials, processes and parameters of manufacturing [23].

Milky patterns and snail trails are defects found on in-field aged PV modules. The presence of a milky pattern was observed in PV modules exposed to 22 years under operating conditions, located mainly near the busbars and the edge of monocrystalline silicon solar cells with a TiO_x antireflective coating [24]. A chemical reaction between the cell titanium oxide layer and the EVA may be the source of this defect [24]. Investigation of moisture ingress in PV modules assembled with multicrystalline Si solar cells with titanium dioxide antireflective layer demonstrated the formation of oxides, hydroxides, sulfides, phosphates, acetates, and carbonates of silver, lead, tin, copper, zinc, and aluminum [25]. The effect of moisture in the solar cells of aged PV modules revealed that the TiO_2 antireflective film was oxidized, highly porous, and aggregated silver nanoparticles [25]. The lamination and soldering processes may also affect the formation of milky patterns.

In snail trails observed in aged PV modules from different module manufacturers, silver carbonate, silver phosphate and silver acetate were found. The exposure to UV irradiation increased the formation of silver acetate in snail tracks [26]. Microanalysis methods were applied to analyze snail trails in multicrystalline Si PV modules removed from three MW-size power plants in operation for 8 years [27]. In the snail trails, Ag-nanoparticles were observed which react with oxygen, CO_2 and the organic encapsulant, forming Ag compounds. Ag_2CO_3 and AgO_2 were the main compounds responsible for the snail-trail discoloration. In the bubbles at the intersection of the Ag paste fingers and the snail trails, CO_2, O_2 and H_2 gases were found [27] and micro-cracks were observed [28]. The material properties of the backsheet can avoid the formation of snail tracks, and the cell metallization process may affect the formation of silver carbonate [26,27]. Moreover,

the analysis with the electroluminescence method led to the conclusion that snail track formation may be related to the PV module assembling and the stress distribution [28].

Considering that in the literature the degradation and aging of PV modules are not related to the silicon solar cell configuration due to the lack of information, this article analyzes and compares the influence of solar cells produced with and without Al-BSF and silicon oxide passivation on the electrical parameter degradation of PV modules, after 77 months under operating conditions in a PV system. Specifically, the I–V curves of two sets of PV modules produced with different solar cell configurations were evaluated before and after outdoor exposure to understand the effect of Al-BSF and emitter passivation with silicon oxide in the degradation rate.

2. Materials and Methods

2.1. Manufacturing Process of Solar Cells and PV Modules

Solar cells and PV modules were developed and manufactured at a pilot plant-scale facility in the early 2000s [29,30]. Two cell-processing sequences were developed to manufacture solar cells with (n^+pp^+) and without (n^+pn^+) Al-BSF using p-type Cz-Si wafers, with a resistivity of 1–10 ohms.cm. Figure 1 compares the two configurations of the developed solar cells. In the Al-BSF devices, the n^+ emitter was passivated with a 10 nm silicon oxide layer. The process to manufacture the n^+pn^+ (without Al-BSF) solar cells was performed with a reduced number of steps and phosphorus diffusion using $POCl_3$.

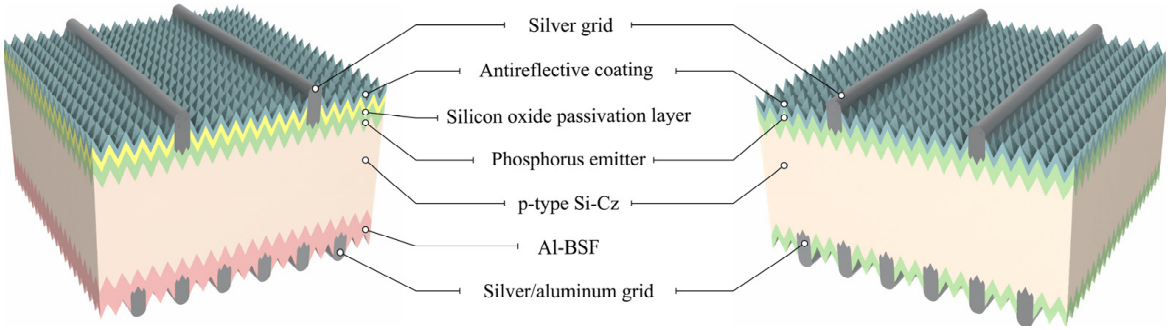


Figure 1. Configuration of the solar cells (**a**) with passivated emitter and Al-BSF (n^+pp^+) and (**b**) without Al-BSF (n^+pn^+), developed at the pilot plant scale.

To develop the passivated emitter and Al-BSF solar cells, the number of steps was increased. After phosphorus diffusion using $POCl_3$, aluminum was deposited using e-beam evaporation and diffused in a quartz tube furnace during the same thermal step to grow a silicon oxide layer of approximately 7 nm for passivating the emitter [30].

The 58 nm thickness of the TiO_2 antireflective coating deposited in n^+pp^+ solar cells was lower than the 68 nm layer formed in n^+pn^+ solar cells, due to the presence of the silicon oxide passivation. Finally, the Ag and Ag/Al grids were screen-printed and fired in a belt furnace, and laser edge isolation was performed. The I–V curve of all produced solar cells was measured under standard conditions, and the solar cells were sorted to manufacture the PV modules [29].

Two groups of PV modules were fabricated with four strings of nine cells and two bypass diodes. The lamination was performed by using high-transparency tempered glass, fast-cure EVA and a white backsheet. The anodized aluminum frames were attached and each module was identified by a barcode. After the assembly, the PV modules were submitted to the standard procedures to measure the I–V curve.

2.2. Characterization of the PV Modules and Degradation Evaluation

Different methods are used to evaluate the failures and degradation in PV modules, such as the I–V curve under standard test conditions, visual inspection, infrared thermog-

raphy, ultraviolet fluorescence, electroluminescence and photoluminescence [17,31]. The I–V curve under standard test conditions (STC) is the method that allows us to obtain the power output at the maximum power point to evaluate the degradation of PV modules. The other techniques may identify a specific failure or degradation.

Before the exposure to outdoor conditions, the I–V curve of all PV modules was measured under STC by using a solar simulator, class AAA. The PV system was installed, and after 77 months, the I–V curves of the two sets of PV modules were measured under the same conditions and equipment used before the exposure to operating conditions. The standard deviation of the maximum power output (P_{MP}) extracted from the I–V characteristic was 4.3×10^{-2}%. Under STC, the standard deviation of the short-circuit current (I_{SC}) was 3.0×10^{-2}%, and it was 2.5×10^{-2}% for the open-circuit voltage (V_{OC}) and fill factor (FF).

The I–V curves were used to evaluate the degradation in percentage and the average annual degradation rate of each electrical parameter of both groups of PV modules. As the materials and procedures used to manufacture the PV modules were the same, the degradation caused by silicon solar cell technology can be compared.

2.3. PV System Description

The PV system was installed in a rooftop building in Rio de Janeiro (latitude = −22.9° and longitude = −43.2°), Brazil. The tilt angle of the 1.89 kW PV array was equal to the latitude. Considering the Köppen–Geiger photovoltaic climatic classification [32], the PV system is located in an AH zone (tropical zone with high irradiation). In Rio de Janeiro, the annual average temperature is 24 °C and the annual average daily total solar irradiation reaching a PV array with a tilt angle equal to the latitude is 5.5 kWh/(m^2·day), as reported by the Brazilian Atlas of Solar Energy.

The PV system was assembled with two strings of PV modules. The 1.1 kW string (SA) was formed by 32 modules assembled with passivated and Al-BSF solar cells, and the 0.79 kW string (SB) was composed of 28 PV modules produced with n^+pn^+ solar cells. The voltage at the maximum power point of string SA and SB was 545 V and 437 V, respectively, and the AC voltage was 220 V. The electric current of each string under STC was 2.07 A (n^+pp^+ solar cells) and 1.95 A (n^+pn^+ solar cells).

3. Results and Discussion

3.1. PV Modules with n^+pn^+ Solar Cells

Figure 2 compares the degradation in percentage of maximum power output, short-circuit current and open-circuit voltage of the PV modules manufactured with solar cells produced without Al-BSF and passivation. In one PV module, the fill factor decreased from 0.77 to 0.66 due to high series resistance, produced by a failure in the solder joint of a ribbon interconnecting strings, and it was excluded from the analysis. Figure 2 shows that the degradation in percentage of the power output was lower than 5.6%, and it was mainly caused by the electric current reduction.

The maximum degradation of the open-circuit voltage was lower than 1%, while the short-circuit current degradation of 5.5% was observed in two modules. All PV modules showed a reduction in the I_{SC}, and in six modules, the V_{OC} remained similar to the initial value. The slight V_{OC} degradation indicates that the minority charge carrier lifetime in the bulk has not degraded, and discarding that, the degradation in the solar cells without Al-BSF assembled in PV modules can be related to the modification of the titanium oxide antireflective coating.

The average, maximum and minimum degradation and the degradation rate of electrical parameters found with the PV modules assembled with n^+pn^+ solar cells are presented in Table 1. The fill factor and V_{OC} presented negligible degradation rates. In the evaluated period, the average degradation of FF and V_{OC} was in the range of 0.5–0.6%.

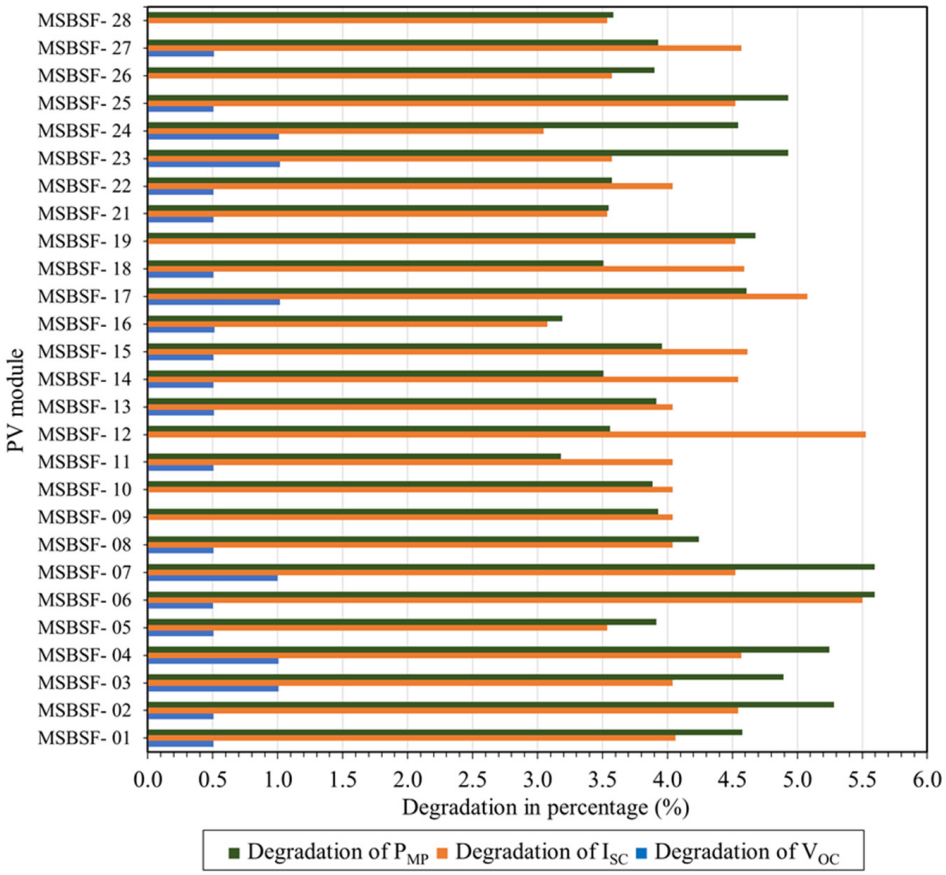


Figure 2. Degradation in percentage of the maximum power output (P_{MP}), short-circuit current (I_{SC}) and open-circuit voltage (V_{OC}) of the PV modules assembled with solar cells without Al-BSF after 77 months in operating conditions in a PV system.

Table 1. Degradation of electrical parameters of PV modules produced with n^+pn^+ solar cells.

Parameter	Average Degradation (%)	Maximum Degradation (%)	Minimum Degradation (%)	Degradation Rate (%/Year)
P_{MP}	4.23	5.59	3.18	0.66
I_{SC}	4.20	5.53	3.05	0.65
V_{OC}	0.51	1.02	0.00	0.08
FF	0.59	1.93	0.00	0.09

The average degradation of the short-circuit current was 4.20% and was similar to the P_{MP} reduction, which was 4.23%. Moreover, Figure 2 shows that the I_{SC} of all PV modules degraded. The minimum and maximum I_{SC} degradation were 3.05% and 5.53%, respectively, and the values were similar to that found for the maximum power output. In the same way, the average degradation rate of the maximum power output (0.66%/year) was similar to that found for the short-circuit current (0.65%/year). These values are lower than those reported in the review presented by Atia et al. [14].

3.2. PV Modules with Passivated Phosphorus-Emitter and Al-BSF Solar Cells

The degradation in percentage of the maximum power output, short-circuit current and open-circuit voltage of the PV modules with passivated front surface and Al-BSF solar cells are shown in Figure 3. In this group, the degradation effect in the I_{SC} also occurred in all modules, and four devices presented a degradation higher than 5%. Nevertheless, the

open-circuit voltage remained the same in 58% of modules, and the degradation observed was lower than 0.5% after 77 months of exposure to outdoor conditions.

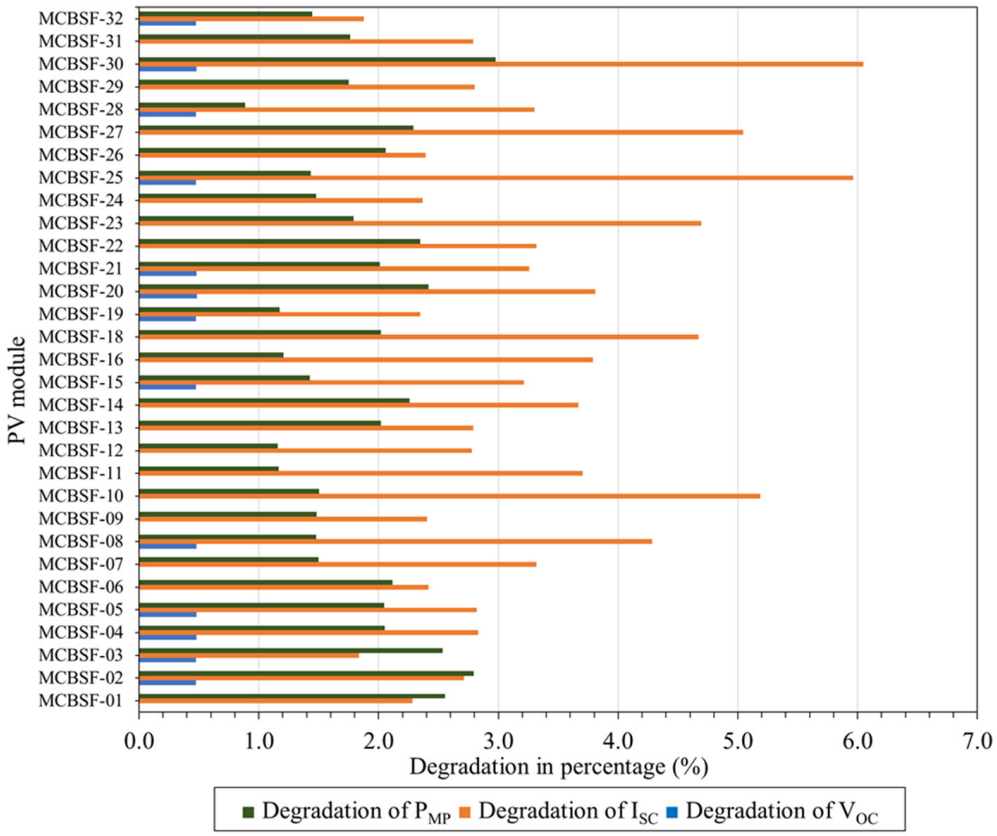


Figure 3. Degradation in percentage of the maximum power output (P_{MP}), short-circuit current (I_{SC}) and open-circuit voltage (V_{OC}) of the PV modules assembled with passivated and Al-BSF solar cells after 77 months in operating conditions.

Concerning the maximum power output, approximately 25% of modules presented a degradation in the percentage in the range of 3–4%. In the other modules, the degradation was lower than these values, but in all devices, the power output decreased.

Table 2 summarizes the degradation of each electrical parameter. As observed in n^+pn^+ solar cell modules, higher degradation was observed in the short-circuit current and the average value was 3.42%. The V_{OC} was slightly reduced, and the average value after 77 months in operating conditions was only 0.2%. Figure 3 shows that in 18 modules, the open-circuit voltage did not change.

Table 2. Degradation of electrical parameters of PV modules assembled with passivated emitter and Al-BSF solar cells.

Parameter	Average Degradation (%)	Maximum Degradation (%)	Minimum Degradation (%)	Degradation Rate (%/Year)
P_{MP}	1.84	2.98	0.89	0.29
I_{SC}	3.42	6.05	1.83	0.53
V_{OC}	0.20	0.48	0	0.03
FF	+1.31	+2.9	0	0.20

In this solar cell configuration, the degradation of the short-circuit current led to a slight increase in the fill factor, with an average value of 1.31% over the period of 77 months. This effect was not observed in the devices without Al-BSF. Regardless, the augment in the

FF is low and may be related to the influence of the Al-BSF or silicon oxide passivation because both groups of modules were characterized under the same conditions. The silicon oxide layer and Al-BSF were produced in the same thermal step. Consequently, in the passivation layer or phosphorus emitter, aluminum atoms may have been introduced, causing an increase in the fill factor with the reduction in short-circuit current.

In this group of PV modules, I_{SC} was also the parameter that led to the maximum power output losses. The average degradation in the P_{MP} was 1.84% and ranged from 0.89% to 2.98%. Consequently, the P_{MP} degradation rate per year was 0.29%.

3.3. Comparison of Degradation in Devices with Different Configurations

Comparing Table 1 with Table 2 and considering that the method and materials used to manufacture the PV modules were the same, the degradation of solar cells with different configurations can be analyzed.

In n^+pp^+ solar cells, the average degradation rate per year of the P_{MP} was around half of that found in n^+pn^+ devices. The low degradation of n^+pp^+ solar cells could be related to the presence of Al-BSF and/or the passivation of the phosphorus emitter with silicon oxide. Specifically, the P_{MP} degradation rate of PV modules with n^+pn^+ solar cells was 0.66% per year, while the devices assembled with passivated emitter and Al-BSF solar cells showed a low degradation rate of 0.29% per year. In both groups of PV modules, the degradation rate is lower than that presented by Lillo-Sánchez et al. [24], which was 1.4% per year after 22 years under outdoor operating conditions.

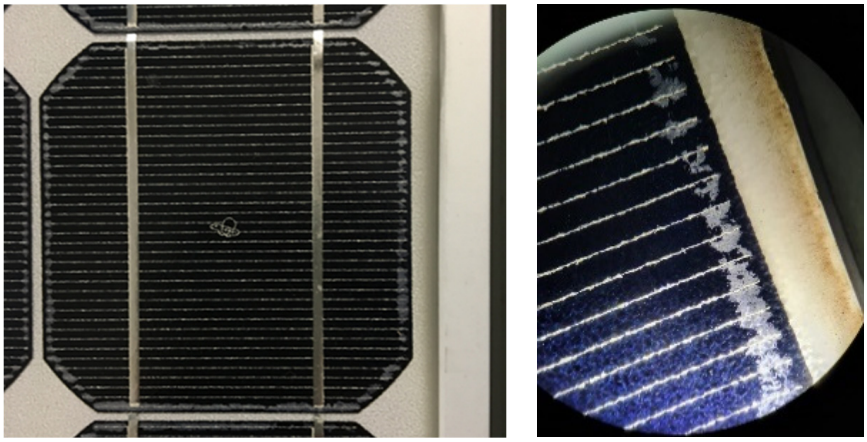
As reported in [24], the reduction in I_{SC} led to the maximum power output losses, but the degradation rate of the short-circuit current was 0.12% per year higher in the devices without Al-BSF and without silicon oxide passivation. The presence of the passivation layer allowed a titanium dioxide antireflective coating 10 nm thinner than that in n^+pn^+ solar cells. The V_{OC} degradation was low in both solar cell configurations. However, the V_{OC} degradation was roughly double in solar cells without Al-BSF and passivation. Considering that the passivation impacts mainly the V_{OC} in silicon solar cells, the passivated solar cells showed a lower V_{OC} degradation rate, caused mainly by the presence of the silicon oxide layer. Based on this result, the PERC configuration, which is manufactured with front and rear passivation, may be a device that will present lower degradation than the early technologies.

A part of the reduction in I_{SC}, observed in both groups of devices, can be related to milky patterns and the snail tracks detected in TiO_2 antireflective coating solar cells, as reported in the literature [24–28,33,34]. The snail tracks were observed in 25% and 29% of the PV modules produced with n^+pn^+ and n^+pp^+ solar cells, respectively. Mik et al. [28] observed a similar result and reported that the number of affected solar cells was almost 30% in the 20 PV modules evaluated. The authors did not find a correlation between the power decrease and the presence of snail tracks and commented that this defect can occur due to chemical reactions between cells, finger grids and/or EVA [28]. Liu et al. [33] concluded that approximately 2% of the power losses are due to the snail trails in PV mini-modules produced with multicrystalline silicon solar cells. This value is similar to the average degradation found in PV modules with a passivated emitter and Al-BSF solar cells.

As reported in the literature [24,34], milky patterns were observed near the edge of all solar cells and in a few devices close to the busbars. Da Fonseca et al. [34] found milky patterns in approximately 80% of the PV modules produced with monocrystalline silicon cells. Lillo-Sánchez and coauthors [24] also observed the presence of the milky pattern mainly near the busbars, in the solar cell edge and, more frequently, in the cells located at the perimeter of the PV module.

Considering the results discussed previously and the locations of the milky patterns observed, this failure can be related to the processing of the solar cells and PV modules. Milky patterns in the TiO_2 antireflective coating might have been formed by the production process of the silicon solar cells. In all cases, milky patterns were noticed near the silver paste fingers at the edge of the solar cells or the busbars, where specific thermal or chemical

processes were carried out. In the solar cells analyzed in this work, the milky pattern defect may have been produced by laser cutting because it was observed mainly close to the silver paste fingers near the edge, as Figure 4 illustrates. The milky pattern may be a phenomenon caused by a chemical reaction of the titanium oxide and the silver paste or an alteration of the crystal structure of the antireflective material influenced by the silver paste and a thermal manufacturing process, such as laser isolation.



(**a**) (**b**)

Figure 4. Illustration of milky pattern in (**a**) the edges of solar cells and (**b**) observed in an optical microscope.

The milky pattern Increased the reflectance of the solar cell due to the shift in the color from blue to white, which contributed to the reduction in I_{SC}. Although the frequency of the milky pattern and affected surface were similar in both groups of devices, the short-circuit current degradation rate of 0.65% per year found in PV modules with n^+pn^+ solar cells was slightly higher than that obtained with passivated emitter and Al-BSF devices, which was 0.53%. This difference was caused by the effect of the emitter passivation with a silicon oxide layer and the Al-BSF, which reduced the I_{SC} degradation rate in silicon solar cells.

4. Conclusions

The electrical parameter degradation of PV modules manufactured with different silicon solar cells were analyzed after 77 months under operating conditions in a PV system installed in Rio de Janeiro, Brazil. The short-circuit current was the parameter that presented higher degradation rate of 0.65% per year and 0.53% per year in PV modules produced without and with Al-BSF solar cells, respectively. The degradation of the I_{SC} led to the maximum power output losses. Therefore, the PV modules assembled with passivated and Al-BSF solar cells showed lower power degradation rate than those produced with n^+pn^+ solar cells. The power degradation rate of the PV modules assembled with passivated emitter n^+pp^+ and n^+pn^+ solar cells was 0.29% per year and 0.66% per year, respectively. The open-circuit voltage reduction was low in both groups of PV devices, but the V_{OC} degradation rate was lower in the PV modules assembled with passivated emitter and Al-BSF solar cells. These results suggest that the PERC configuration can degrade less than the early technologies due to the influence of silicon oxide passivation.

The degradation of short-circuit current can be related to the titanium dioxide antireflective coating. The reduction in the electric current was slightly lower in the solar cells with silicon oxide passivation because the thickness of the titanium dioxide layer was around 10 nm thinner than that deposited in n^+pn^+ solar cells.

Snail tracks were observed in 29% and 25% of the PV modules with Al-BSF and n^+pn^+ solar cells, respectively, but the milky pattern was observed in all PV modules. As reported in the literature, the presence of the milky pattern was observed in solar cells produced with the titanium dioxide antireflective coating. The milky pattern can be a phenomenon caused

by chemical reactions of the titanium oxide, silver paste and EVA or a modification of the crystal structure of the antireflective material influenced by the silver paste and a thermal manufacturing process. In the solar cells developed, laser isolation may be responsible for producing the milky pattern. To avoid or prevent milky pattern and snail track formation, the solar cell and PV module processing should be optimized and the combination of materials used to form the antireflective coating, metal grid and encapsulation should be investigated.

In addition to the materials, the processes to produce the silicon solar cells influence the degradation of the PV modules, elucidating the large diversity of results reported in the literature about degradation and failures. Beyond the monocrystalline or multicrystalline substrate, other factors affect the aging of silicon solar cells in PV modules exposed to outdoor conditions, but this information is usually not disclosed by the manufacturer. Therefore, as silicon solar cell and PV module technology evolves, failures and degradation become more complex, and specific analysis is needed. The investigation of PV modules aging of diverse solar cell technologies is a broad field and, as future research, the degradation of PV modules as a function of time period of exposure to outdoor and operating condition can be evaluated for different solar cell configurations [35]. Moreover, the aging of new technologies such perovskite-Si tandem solar cells should be explored [36].

Author Contributions: I.Z. and A.M. established the research direction of the paper and wrote the main part of the paper. J.F. and J.V.Z.B. provided the experimental data curation and analyzed the results. M.L. and B.I.d.S.R.L. conducted and analyzed the I–V characteristic measurements. T.C.P. contributed to establishing the state of the art of PV module degradation and analyzing experimental results. All authors have read and agreed to the published version of the manuscript.

Funding: This research was funded by Financiadora de Estudos e Projetos (FINEP), grant number 01.22.0194.00 and 01.04.0651.00; and Petrobras—Petróleo Brasileiro S. A., Eletrosul—Centrais Elétricas S. A., Companhia Estadual de Geração e Transmissão de Energia Elétrica (CEEE-GT). The APC was funded by FINEP.

Data Availability Statement: Data are contained within the article.

Acknowledgments: The authors acknowledge the staff of NT-Solar/PUCRS engaged in processing and characterizing the silicon solar cells and PV modules.

Conflicts of Interest: The authors declare no conflicts of interest. The funders had no role in the design of the study; in the collection, analyses, or interpretation of data; in the writing of the manuscript; or in the decision to publish the results.

References

1. VDMA. *The International Technology Roadmap for Photovoltaic (ITRPV)*, 8th ed.; VDMA: Frankfurt, Germany, 2017; p. 39.
2. VDMA. *The International Technology Roadmap for Photovoltaic (ITRPV)*, 14th ed.; VDMA: Frankfurt, Germany, 2023; p. 81.
3. REN21. *Renewables 2020 Global Status Report*; REN21: Paris, France, 2020; p. 367.
4. Green, M.A. The Passivated Emitter and Rear Cell (PERC): From conception to mass production. *Sol. Energy Mater. Sol. Cells* **2015**, *143*, 190–197. [CrossRef]
5. Blakers, A.W.; Wang, A.; Milne, A.M.; Zhao, J.; Green, M.A. 22.8% efficient silicon solar cell. *Appl. Phys. Lett* **1989**, *55*, 1363–1365. [CrossRef]
6. Wang, A.; Zhao, J.; Green, M.A. 24% efficient silicon solar cells. *Appl. Phys. Lett.* **1990**, *57*, 602–604. [CrossRef]
7. Ballif, C.; Haug, F.J.; Boccard, M.; Verlinden, P.J.; Hahn, G. Status and perspectives of crystalline silicon photovoltaics in research and industry. *Nat. Rev. Mater.* **2022**, *7*, 597–616. [CrossRef]
8. Lim, J.R.; Shin, W.G.; Lee, C.G.; Lee, Y.G.; Ju, Y.C.; Ko, S.W.; Kim, J.D.; Kang, G.H.; Hwang, H. A Study of the Electrical Output and Reliability Characteristics of the Crystalline Photovoltaic Module According to the Front Materials. *Energies* **2021**, *14*, 163. [CrossRef]
9. Guerra, M.R.; Laita, Í.P.; Solano, M.G.; Pascual, J. In-field energy performance of solar PV module made of UMG silicon. *IEEE J. Photovolt.* **2022**, *12*, 1109–1115. [CrossRef]
10. Kaaya, I.; Ascencio-Vásquez, J.; Weiss, K.-A.; Topič, M. Assessment of uncertainties and variations in PV modules degradation rates and lifetime predictions using physical models. *Sol. Energy* **2021**, *218*, 354–367. [CrossRef]
11. Aghaei, M.; Fairbrother, A.; Gok, A.; Ahmad, S.; Kazim, S.; Lobato, K.; Oreski, G.; Reinders, A.; Schmitz, J.; Theelen, M.; et al. Review of degradation and failure phenomena in photovoltaic modules. *Renew. Sustain. Energy Rev.* **2022**, *159*, 112160. [CrossRef]

12. De Oliveira, M.C.C.; Cassini, D.A.; Diniz, A.S.A.C.; Soares, L.G.; Viana, M.M.; Kazmerski, L.L.; Lins, V.D.F.C. Comparison and analysis of performance and degradation differences of crystalline-Si photovoltaic modules after 15-years of field operation. *Sol. Energy* **2019**, *191*, 235–250. [CrossRef]
13. Kahoul, N.; Cheghib, H.; Sidrach-de-Cardona, M.; Affari, B.C.; Younes, M.; Kherici, Z. Performance degradation analysis of crystalline silicon solar cells in desert climates. *Energy Sustain. Dev.* **2021**, *65*, 189–193. [CrossRef]
14. Atia, D.M.; Hassan, A.A.; El-Madany, H.T.; Eliwa, A.Y.; Zahran, M.B. Degradation and energy performance evaluation of mono-crystalline photovoltaic modules in Egypt. *Sci. Rep.* **2023**, *13*, 13066. [CrossRef]
15. Belhaouas, N.; Mehareb, F.; Kouadri-Boudjelthia, E.; Assem, H.; Bensalem, S.; Hadjrioua, F.; Aissaoui, A.; Hafdaoui, H.; Chahtou, A.; Bakria, K.; et al. The performance of solar PV modules with two glass types after 11 years of outdoor exposure under the mediterranean climatic conditions. *Sustain. Energy Technol. Assess.* **2022**, *49*, 101771. [CrossRef]
16. Luo, W.; Clement, C.E.; Khoo, Y.S.; Wang, Y.; Khaing, A.M.; Reindl, T.; Kumar, A.; Pravettoni, M. Photovoltaic module failures after 10 years of operation in the tropics. *Renew. Energy* **2021**, *177*, 327–335. [CrossRef]
17. Koester, L.; Lindig, S.; Louwen, A.; Astigarraga, A.; Manzolini, G.; Moser, D. Review of photovoltaic module degradation, field inspection techniques and techno-economic assessment. *Renew. Sustain. Energy Rev.* **2022**, *165*, 112616. [CrossRef]
18. Jordan, D.C.; Silverman, T.J.; Wohlgemuth, J.H.; Kurtz, S.R.; VanSant, K.T. Photovoltaic failure and degradation modes. *Prog. Photovolt.: Res. Appl.* **2017**, *25*, 318–326. [CrossRef]
19. Lindig, S.; Kaaya, I.; Weiss, K.-A.; Moser, D.; Topic, M. Review of Statistical and Analytical Degradation Models for Photovoltaic Modules and Systems as Well as Related Improvements. *IEEE J. Photovolt.* **2018**, *8*, 1773–1786. [CrossRef]
20. Chowdhury, M.S.; Rahman, K.S.; Chowdhury, T.; Nuthammachot, N.; Techato, K.; Akhtaruzzaman, M.; Tiong, S.K.; Sopian, K.; Amin, N. An overview of solar photovoltaic panels' end-of-life material recycling. *Energy Strategy Rev.* **2020**, *27*, 100431. [CrossRef]
21. Herguth, A.; Hahn, G. Kinetics of the boron-oxygen related defect in theory and experiment. *J. Appl. Phys.* **2010**, *108*, 114509. [CrossRef]
22. Markevich, V.P.; Vaqueiro-Contreras, M.; De Guzman, J.T.; Coutinho, J.; Santos, P.; Crowe, I.F.; Halsall, M.P.; Hawkins, I.; Lastovskii, S.B.; Murin, L.I.; et al. Boron–Oxygen Complex Responsible for Light-Induced Degradation in Silicon Photovoltaic Cells: A New Insight into the Problem. *Phys. Status Solidi A* **2019**, *216*, 1900315. [CrossRef]
23. Bredemeier, D.; Walter, D.; Herlufsen, S.; Schmidt, J. Lifetime degradation and regeneration in multicrystalline silicon under illumination at elevated temperature. *AIP Adv.* **2016**, *6*, 035119. [CrossRef]
24. Lillo-Sánchez, L.; López-Lara, G.; Vera-Medina, J.; Pérez-Aparicio, E.; Lillo-Bravo, I. Degradation analysis of photovoltaic modules after operating for 22 years. A case study with comparisons. *Sol. Energy* **2021**, *222*, 84–94. [CrossRef]
25. Segbefia, O.K.; Akhtar, N.; Sætre, T.O. Moisture induced degradation in field-aged multicrystalline silicon photovoltaic modules. *Sol. Energy Mater. Sol. Cells* **2023**, *258*, 112407. [CrossRef]
26. Duerr, I.; Bierbaum, J.; Metzger, J.; Richter, J.; Philipp, D. Silver grid finger corrosion on snail track affected PV modules—Investigation on degradation products and mechanisms. *Energy Procedia* **2016**, *98*, 74–85. [CrossRef]
27. Filho, N.M.; Diniz, A.S.A.C.; Vasconcelos, C.K.B.; Kazmerski, L.L. Snail trails on PV modules in Brazil's tropical climate: Detection, chemical Properties, bubble formation, and performance effects. *Sustain. Energy Technol. Assess.* **2022**, *54*, 102808. [CrossRef]
28. Mik, K.; Bugaj, M.; Chaja, P. The evaluation of the snail track affected photovoltaic modules by different methods after 3-year operating in central Poland. *Renew. Energy* **2021**, *163*, 504–516. [CrossRef]
29. Moehlecke, A.; Zanesco, I. Pilot plant to develop cost effective photovoltaic modules. In Proceedings of the 22nd EU PVSEC, Milan, Italy, 3–7 September 2007; pp. 1772–1775.
30. Moehlecke, A.; Zanesco, I. Development of silicon solar cells and photovoltaic modules in Brazil: Analysis of a pilot production. *Mat. Res.* **2012**, *15*, 581–588. [CrossRef]
31. Spataru, S.; Hacke, P.; Sera, D. In-Situ Measurement of Power Loss for Crystalline Silicon Modules Undergoing Thermal Cycling and Mechanical Loading Stress Testing. *Energies* **2021**, *14*, 72. [CrossRef]
32. Ascencio-Vásquez, J.; Brecl, K.; Topič, M. Methodology of Köppen–Geiger–Photovoltaic climate classification and implications to worldwide mapping of PV system performance. *Sol. Energy* **2019**, *191*, 672–685. [CrossRef]
33. Liu, H.; Huang, C.; Lee, W.; Yan, S.; Lin, F. A Defect Formation as Snail Trails in Photovoltaic Modules. *Energy Power Eng.* **2015**, *7*, 348–353. [CrossRef]
34. Da Fonseca, J.E.F.; De Oliveira, F.S.; Prieb, C.W.M.; Krenzinger, A. Degradation analysis of a photovoltaic generator after operating for 15 years in southern Brazil. *Sol. Energy* **2020**, *195*, 196–206. [CrossRef]
35. Kaaya, I.; Lindig, S.; Weiss, K.A.; Virtuani, A.; Ortin, M.S.C.; Moser, D. Photovoltaic lifetime forecast model based on degradation patterns. *Prog. Photovolt. Res. Appl.* **2020**, *28*, 979–992. [CrossRef]
36. Liu, N.; Wang, L.; Xu, F.; Wu, J.; Song, T.; Chen, Q. Recent Progress in Developing Monolithic Perovskite/Si Tandem Solar Cells. *Front. Chem.* **2020**, *8*, 603375. [CrossRef] [PubMed]

Disclaimer/Publisher's Note: The statements, opinions and data contained in all publications are solely those of the individual author(s) and contributor(s) and not of MDPI and/or the editor(s). MDPI and/or the editor(s) disclaim responsibility for any injury to people or property resulting from any ideas, methods, instructions or products referred to in the content.